Enantiospecific Orientation of *R*–3-Methylcyclohexanone on the Chiral Cu(643)$^{R/S}$ Surfaces

Joshua D. Horvath,† Layton Baker,† and Andrew J. Gellman*,†,‡

Department of Chemical Engineering, Carnegie Mellon University, Pittsburgh, Pennsylvania 15213, and National Energy Technology Laboratory, U.S Department of Energy, P.O. Box 10940, Pittsburgh, Pennsylvania

Received: July 10, 2007; Revised Manuscript Received: March 6, 2008

The high Miller index planes of metal single crystals are chiral, if they do not lie perpendicular to any of the mirror symmetry planes of the bulk lattice. Such chiral surfaces of face-centered cubic metals expose kinked step edges and have been shown to have enantiospecific interactions with chiral adsorbates. *R*–3-methylcyclohexanone (*R*-3MCHO) exhibits enantiospecific differences in its desorption energies from the *R* and *S* chiral kinks on the Cu(643)$^{R/S}$ surfaces. This enantiospecific interaction must also manifest itself in the orientations of *R*-3MCHO adsorbed at chiral kinks and has been probed by examining the intensities of infrared absorption by *R*-3MCHO adsorbed at the kinks on the Cu(643)$^{R/S}$ surfaces. Fourier transform infrared reflection−absorption spectra show that the interaction of the *R*-3MCHO occurs through the carbonyl group which exhibits a red-shift in its stretching mode as a result of adsorption on the surface. The absorption intensities also indicate that the molecule is oriented with the >C═O bond roughly parallel to the surface. More importantly, *R*-3MCHO adsorbed at the *R* and the *S* kinks on the Cu(643)$^{R/S}$ surfaces exhibits different relative absorption intensities of its vibrational modes, clearly indicating that the orientations of *R*-3MCHO are enantiospecific on the two enantiomorphic surfaces.

1. Introduction

Chiral surfaces have enormous potential application in enantioselective chemical processing. The most common chiral surfaces used in enantioselective chromatography and as enantioselective catalysts are based on achiral surfaces that have been templated by the adsorption of chiral organic ligands. It is also possible to produce naturally chiral solid surfaces from both chiral and achiral crystalline materials. For example, a chiral surface is generated when achiral face-centered cubic (fcc) crystalline metals are cut to expose surface structures with kinked steps separating low Miller index terraces. McFadden et al. first pointed out that the (643) and ($\bar{6}4\bar{3}$) surfaces of a fcc crystal are nonsuperimposable mirror images of one another and thus chiral.[1] A naming convention has since been adopted which denotes such surfaces and their chirality as either (643)^S or (643)^R.[2,3] Such chiral solid surfaces exhibit enantioselectivity in the presence of chiral adsorbates.[2–19]

Enantiospecificity on chiral surfaces can take the form of enantiospecific desorption energies, reaction rates, reaction selectivities, and enantiospecific adsorbate geometries. Several theoretical and experimental studies of the interactions of chiral fcc surfaces with chiral adsorbates have revealed enantiospecific desorption energies and reaction rates.[2–13,20] In addition, there are a couple of experiments that have examined the orientations of chiral molecules on naturally chiral metal surfaces. The first such experiment used Fourier-transform infrared reflection−absorption spectra (FT-IRAS) to demonstrate that the orientations of *R*- and *S*-2-butanoxy groups on the Ag(643)^R surface are enantiospecific.[6] In spite of the fact that the orientations of the chiral 2-butoxides on the Ag(643)^R surface are enantiospecific, the barriers to their reaction by β-hydride elimination did not exhibit measurable enantiospecificity. A more recent study has made use of X-ray photoelectron diffraction and density functional theory to demonstrate that the orientations of D- and L-cysteine on the Au(17, 11, 9)^S surface are enantiospecific.[16] In addition, there are several computational predictions that amino acids should adopt enantiospecific geometries on naturally chiral surfaces.[17–19]

R–3-Methylcyclohexanone (hereafter referred to as *R*-3MCHO) is the chiral adsorbate that has been studied to the greatest extent on naturally chiral metal surfaces, and it has been shown that the desorption energies of *R*-3MCHO from the chiral kinks on the Cu(643)$^{R/S}$ surfaces are enantiospecific. Figure 1 illustrates the molecular structure of *R*-3MCHO and depicts it adsorbed at the kink sites on the ideal Cu(643)^S surface. The work presented here uses FT-IRAS to demonstrate that the adsorption geometries of *R*-3MCHO are enantiospecific when it is adsorbed at the kinks on the Cu(643)$^{R/S}$ surfaces.

Previous work has used temperature programmed desorption (TPD) to demonstrate that the desorption kinetics of *R*-3MCHO from the kinks on the Cu(643)$^{R/S}$ surfaces are enantiospecific and reflect an enantiospecific difference in its desorption energies, $\Delta E^{\ddagger}_{des}$, from the kinks on the two surfaces.[6,8,9] Such enantiospecific $\Delta E^{\ddagger}_{des}$ could be caused by the chiral *R*-3MCHO "fitting" into the S-kinks on the Cu(643)^S surface better than it "fits" into the *R* kinks on the Cu(643)^R surfaces. Although enantiospecific adsorption of chiral adsorbates on naturally chiral metal surfaces must be a general phenomenon, this preference of the *R* enantiomer for the *S* kinks is not expected to be general. The enantiospecificity of the interaction of *R*-3MCHO with the Cu(643)$^{R/S}$ surfaces must result in its adopting different adsorption geometries which ought to be detectable by FT-IRAS.

Infrared absorption by molecules adsorbed on surfaces is typically used to identify species on the basis of their vibrational mode frequencies. FT-IRAS is also, however, a very sensitive probe of the orientation of adsorbed molecules. In the gas phase or in solution, molecules are randomly oriented and the intensity of a given vibrational mode is dictated only by the magnitude

* Corresponding author (412-268-3848, gellman@cmu.edu).
† Carnegie Mellon University.
‡ National Energy Technology Laboratory.

10.1021/jp0753878 CCC: $40.75
Published on Web 04/30/2008

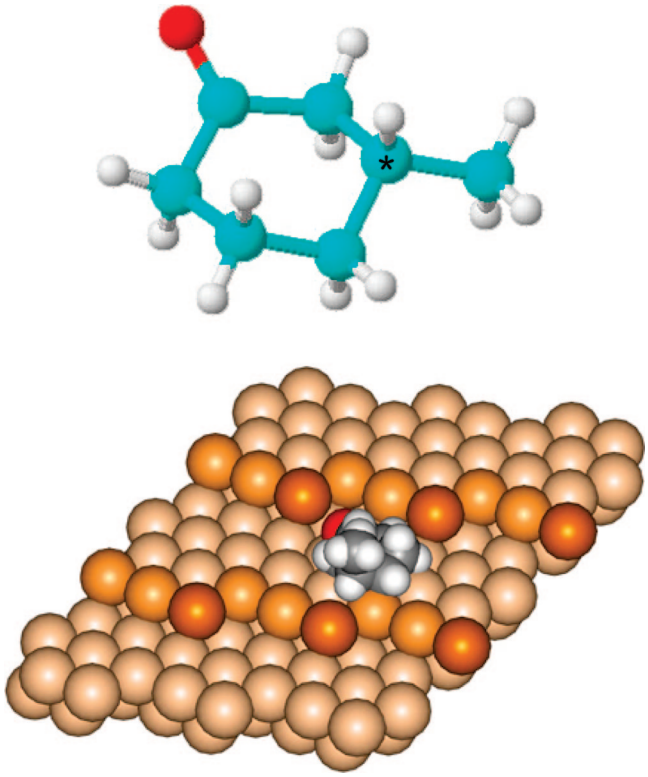

Figure 1. Isolated *R*-3MCHO and a model of *R*-3MCHO adsorbed onto an ideal Cu(643)^S surface. The schematic of the adsorbed *R*-3MCHO is intended to indicate the relative sizes of the molecule and the ideal unit cell. The orientation shown in the figure has the >C═O bond and molecular ring roughly parallel to the surface and is consistent with the results of the FT-IRAS spectra obtained at low coverages. The adsorption site at low coverages is the kink but the details of the positioning at the kink are unknown.

of its dynamic dipole monument, $\vec{\mu}$. Once adsorbed on a surface, however, molecules are aligned in space. Furthermore, at a metal surface the electric field vector of infrared radiation reflected from the surface is aligned along the surface normal, $\hat{n}$. The intensity of absorption is then given by

$$I \propto (\vec{\mu}\hat{n})^2 \quad (1)$$

As a result, the intensity of absorption by an adsorbate vibrational mode varies with orientation as $\cos^2\theta_{\vec{\mu}\hat{n}}$ where $\theta_{\vec{\mu}\hat{n}}$ is the angle between the dynamic dipole moment and the surface normal. Thus, the intensities of the absorption features in FT-IRAS are very sensitive to the orientation of the adsorbate with respect to the surface normal.

This paper describes the FT-IRAS spectra of *R*-3MCHO and racemic 3MCHO adsorbed on the chiral Cu(643)$^{R/S}$ surfaces. 3MCHO can adsorb on the Cu(643) surfaces at three distinct sites: the (111) terraces, the straight step edges, and the kinks. The $\Delta E^{\ddagger}_{des}$ of 3MCHO from the terraces, step edges, and kinks are 61, 93, and 104 kJ/mol, respectively.[8] Desorption from the kinks has been shown to be enantiospecific with a difference in desorption energies of $\Delta\Delta E^{\ddagger}_{des} = 1$ kJ/mol for *R*-3MCHO on the *R* and *S* kinks. FT-IRAS spectra were collected at coverages which saturated the kinks, coverages which saturated both the steps and the kinks, and then coverages which saturated the entire surface. The intensities of the IR spectra vary as a function of coverage, indicating that the average 3MCHO orientation changes as the coverage increases. More importantly, the FT-IRAS data reveal that the orientations of *R*-3MCHO adsorbed at kink sites on the Cu(643)$^{R/S}$ surfaces are enantiospecific.

2. Experimental Section

The FT-IRAS spectra were obtained using an FTIR spectrometer interfaced to an ultrahigh vacuum chamber. IR radiation from a commercial FT-IR spectrometer (Mattson model RS-10000) entered the UHV chamber through a 1.5-in. diameter plano-convex ZnSe lens with a 12-in. focal length. The ZnSe (Janos Technology) lens has a broadband antireflective coating that provided 95% transmission over the 3.5−13.0 μm wavelength range. The lens focused the IR beam onto the sample at grazing incidence (85°). It was reflected by the polished metal crystal and exited the chamber through an identical plano-convex ZnSe lens. After exiting the chamber, the parallel beam was focused by a parabolic polished aluminum mirror with a 10 in. focal length onto an elliptical mirror which redirected the beam onto the external, liquid nitrogen cooled mercury−cadmium−telluride (MCT) IR detector.

The Cu(643) sample was polished on both sides to expose the Cu(643)^R and Cu(643)^S surfaces. Initially, extensive sputtering and annealing cycles were needed to remove impurities. This involved Ar^+ bombardment with a current of approximately 20 μA at 1.5 keV. The sample was annealed to 1000 K for 300 s every 15 min while sputtering the surface. To obtain clean and ordered Cu(643)$^{R/S}$ surfaces, each side of the crystal received 25 h of Ar^+ ion sputtering. Surface cleanliness was verified by Auger electron spectroscopy and the surface structure was verified by observation of sharp low-energy electron diffraction patterns. To remove carbon contamination and ensure identical surface conditions for each experiment, the surfaces were cleaned by Ar^+ sputtering and annealing after each *R*-3MCHO adsorption and desorption cycle.

R-3MCHO and 3MCHO were obtained from Aldrich and were transferred to glass vials and subjected to several cycles of freezing, pumping, and thawing to remove air and other high vapor pressure impurities prior to use. The purity of each sample was verified by mass spectrometry. Exposure of the sample surfaces to the chiral compounds was performed by introducing the vapor into the UHV chamber through a leak valve while measuring the chamber pressure with the ion gauge. Exposures are reported in Langmuirs (1 L = 10^{-6} Torr s) and are not corrected for ion gauge sensitivity to different gas species. To limit adsorption of the 3MCHO to the just the kinks, to both the kinks and the steps, or to a monolayer across the entire surface, the sample temperature was held at 320, 240, or 185 K, respectively, during exposure to 3MCHO vapor.

RAIRS data were collected as double-sided interferograms with a forward/reverse mirror speed of 3.2 cm/s and 4 cm^{-1} resolution. The clean sample was positioned in the IR beam, and the detector signal was maximized by adjusting the sample and detector positions. Once the sample was in position, the spectrometer collected 5000 background scans in approximately 24 min. The sample was held at 250 K to prevent CO adsorption during collection of the background spectra. After the background data were collected, the crystal was exposed to the 3MCHO without repositioning the sample. Exposure of the surface to adsorbates was achieved by background exposure or by direct exposure using a dosing tube and leak valve mounted on a linear translator. This linear translator allowed the dosing tube to be positioned extremely close to the sample to achieve high coverages with very low exposures. After adsorption, 5000 scans of the adsorbate-covered surface were collected in

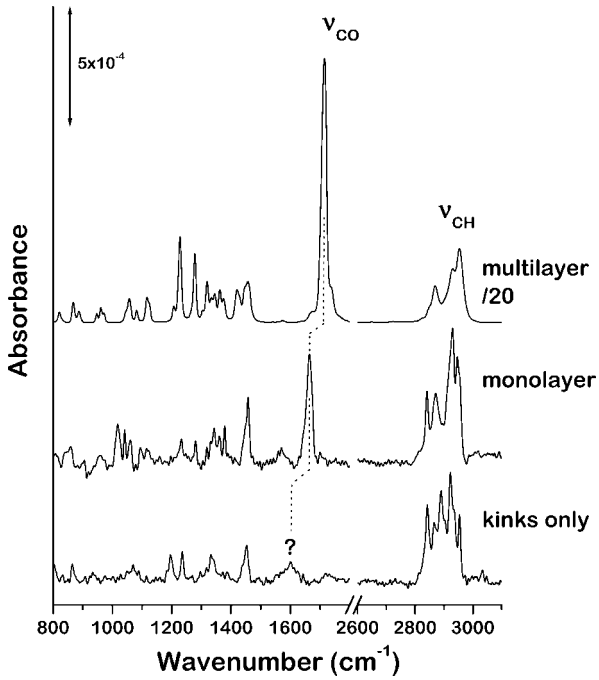

Figure 2. FT-IRAS spectra of *R*-3MCHO on Cu(643)^{R} at 0.35 monolayer coverage (kinks only), 1.0 monolayer, and ~100 monolayers. A number of the absorption bands in the regions around 1000−1800 and 2800−3000 cm^{-1} have intensities which vary as a function of coverage. This indicates that the average orientation of *R*–3-MCHO molecules on the surface varies as a function of coverage. The redshift of the $\upsilon_{C=O}$ frequency in the monolayer and submonolayer regimes suggests that the >C═O bond is interacting with the surface. Spectra have been offset for clarity.

approximately 24 min. After collecting the RAIRS data, the adsorbate-covered sample was positioned in front of the mass spectrometer and a temperature programmed desorption experiment was performed to determine the coverage of the adsorbate.

3. Results

3.1. 3-MCHO Interaction with Cu(643). The Cu(643)$^{R/S}$ surfaces expose kink sites, straight step edges and (111) terraces for adsorption of 3MCHO (Figure 1). It is reasonable to expect that the adsorption geometry or orientation will depend on the nature of the adsorption site and that the adsorption geometry is enantiospecific at the chiral kink sites. Reflection−absorption infrared spectra were collected for *R*-3MCHO and racemic 3MCHO on the Cu(643)$^{R/S}$ surfaces. Spectra were obtained at adsorbate coverages of 0.35, 0.7, 1.0, and 100 monolayers. In this case, a monolayer is defined as the coverage above which one begins to observe multilayer desorption in the TPD spectra. An exposure of 0.15 L at 320 K resulted in a coverage of 0.35 monolayer with only the kink sites filled.[8,9,14,15] At 320 K the desorption of 3MCHO from the straight step edges or from the terrace sites is very rapid and so, adsorption is restricted to the kink sites. A coverage of 0.70 monolayer was achieved by exposing the surfaces to 0.15 L at 240 K, filling both the kink and straight step sites. The 1 monolayer coverage resulted from an exposure of 0.15 L at 185 K and filled the terrace, straight step, and kink sites on the surface. Exposing the surface to 2.0 L of 3MCHO at 90 K resulted in a coverage of ~100 monolayers.

Examination of the FT-IRAS spectra provides insight into the orientation of 3MCHO on the surface and into the origin of its interaction with the Cu(643)$^{R/S}$ surfaces when adsorbed at the different types of sites. Figure 2 shows the FT-IRAS spectra of *R*-3MCHO adsorbed at the kinks only (0.35 ML) and at coverages of 1.0 monolayer and 100 monolayers. The FT-IRAS spectrum of the multilayer closely resembles the reference spectra for 3MCHO[21] and cyclohexanone.[22–24] The structure of 3-MCHO is complicated, and as a result, the IR vibrational assignments are not straightforward and a detailed assignment is beyond the scope of this work. The modes observed in the 2800−3100 cm^{-1} region are easily assignable to the CH_2 and CH_3 stretches. The carbonyl stretching mode was easily identifiable at 1715 cm^{-1} in the multilayer spectrum. The modes observed at lower frequencies arise from complicated motions of the ring and from deformation of the CH_2 and CH_3 groups.

Numerous changes are observed in the vibrational spectra of *R*-3MCHO on the Cu(643)$^{R/S}$ surface as the coverage decreases. Figure 2 shows the FT-IRAS spectra for *R*-3MCHO on the Cu(643)^{R} surface as a function of coverage. When the coverage is reduced to 1 monolayer, the $\upsilon_{C=O}$ mode observed at 1715 cm^{-1} in the multilayer is red-shifted to 1664 cm^{-1} and has been reduced in intensity by a factor of 5 relative to the intensity of the CH stretch modes. After the coverage has been reduced to 0.35 monolayers, the coverage at which the *R*-3MCHO is adsorbed at the kinks only, the frequency of the $\upsilon_{C=O}$ mode is reduced to ~1600 cm^{-1}, and the feature has been reduced in intensity by another factor of 5 relative to the CH stretch modes. Also note that the $\upsilon_{C=O}$ mode feature has become significantly broadened. There are many other obvious changes to the FTIR spectrum of *R*-3MCHO as its coverage is reduced from 100 to 0.35 ML. It is important to note that these changes are not associated with decomposition of *R*-3MCHO on the surface as the molecule desorbs intact during heating. It is most likely that they are due to intensity variations as the average orientation of the adsorbate changes with coverage.

The red-shifting of the $\upsilon_{C=O}$ mode frequency in the *R*-3MCHO from 1715 cm^{-1} in the multilayer to 1664 cm^{-1} in the monolayer adsorbed on the Cu(643) surface suggests that the >C═O group is largely responsible for the interaction of the *R*-3MCHO with the surface. Similar red-shifts in $\upsilon_{C=O}$ mode have been observed as a result of the adsorption of acetone on the Au(111) and Pt(111) surfaces.[25,26] On the Au(111) surface the $\upsilon_{C=O}$ mode of acetone shifts from 1712 cm^{-1} in the multilayer to 1669 cm^{-1} in the adsorbed monolayer.[25] On the Pt(111) surface the $\upsilon_{C=O}$ mode of acetone shifts from 1719 cm^{-1} in the multilayer to 1642 cm^{-1} in the adsorbed monolayer.[26] This type of red-shifting is commonly ascribed to donation of electrons from the >C═O group to the surface, resulting in a fairly strong interaction with the surface but a weakening of the >C═O bond in the adsorbate.

The intensity of the $\upsilon_{C=O}$ mode relative to the intensity of the CH stretch modes is obviously reduced in the monolayer and sub-monolayer states relative to that the multilayer state. In the multilayer state the molecules are randomly oriented, whereas in the monolayer and submonolayer states the *R*-3MCHO is oriented by the surface. The most likely origin of the reduced intensity of the $\upsilon_{C=O}$ mode in the adsorbed molecules is that the >C═O bond is oriented roughly parallel to the surface and thus its absorption intensity is reduced. In the sub-monolayer state with the *R*-3MCHO adsorbed only at the kinks, the $\upsilon_{C=O}$ mode intensity is even further reduced from that in the adsorbed monolayer. The orientation of the molecule with the >C═O bond parallel to the surface is consistent with an adsorption geometry in which the cyclohexanone ring is oriented parallel to the surface, as suggested in the illustration of Figure 1. It is important to note, however, that the illustration in Figure 1 is not based on any quantitative prediction of the

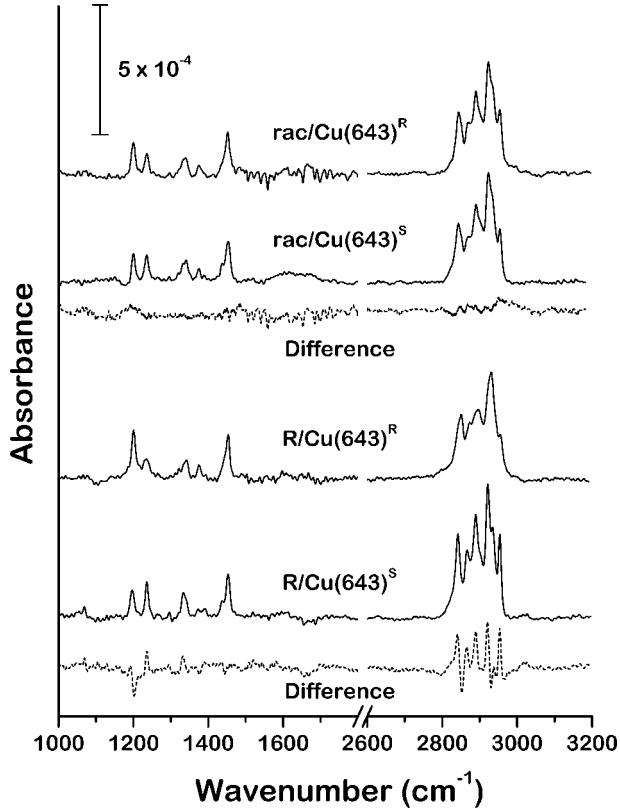

Figure 3. Comparison of racemic 3MCHO and *R*-3MCHO on Cu(643)$^{R/S}$ surfaces. The FT-IRAS spectra of rac-3MCHO are identical on both chiral surfaces, as indicated by the difference spectrum (dashed line). In contrast, there are significant differences between the FT-IRAS spectra of *R*-3MCHO on Cu(643)$^{R/S}$ surfaces. This difference in FT-IRAS absorption intensities indicates that the *R*-3MCHO adopts different orientations on the two surfaces. Spectra have been offset for clarity.

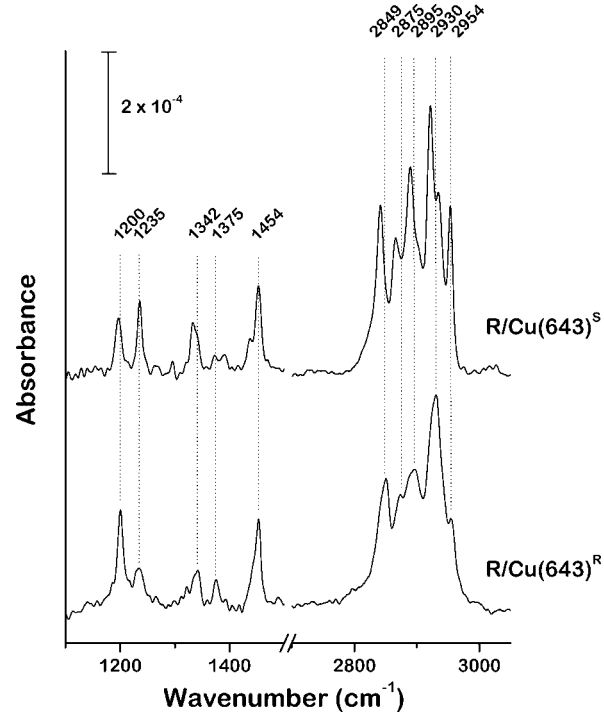

Figure 4. FT-IRAS spectra of 0.35 monolayers of *R*-3MCHO adsorbed only at the kink sites on Cu(643)$^{R/S}$ surfaces. These spectra highlight the differences in the 1150−1450 and 2750−3050 cm^{-1} regions of the spectra. While some features appear to be slightly shifted with respect to one another it is possible that this is simply due to changes in the intensities of adjacent, unresolved peaks. The primary differences between the spectra are the relative intensities of the absorption features associated with various modes.

orientation and furthermore and that the FT-IRAS spectra themselves give no indication of the adsorption site.

A final point to note is that the $\upsilon_{C=O}$ mode in the *R*-3MCHO adsorbed at the kink sites is quite broad. As has been noted in several previous publications, the real structure of the Cu(643)$^{R/S}$ surfaces is much more complex than that of the ideal surface. Diffusion of atoms along the step edges results in the coalescence of kinks and the formation of roughened step edges with a variety of types of kink structures.[3,11,27,28] This has been predicted by simulation and observed by scanning tunneling microscopy.[29] The fact that the step edges are roughened results in the presence of a variety of different kink adsorption sites for *R*-3MCHO. The breadth of the FT-IRAS absorption feature assigned to *R*-3MCHO at the kink sites may be attributable to the heterogeneity of the kink sites giving rise to inhomogeneous broadening of the $\upsilon_{C=O}$ mode.

3.2. Enantiospecific Orientation of *R*-3MCHO on Cu(643)$^{R/S}$. Detection of the enantiospecific adsorption of *R*-3MCHO at the *R* and *S* kinks on the Cu(643)$^{R/S}$ surfaces requires comparison of the FT-IRAS absorption intensities of *R*-3MCHO adsorbed at these sites. In order to be certain that any detected differences are truly due to enantiospecificity, one must first compare the FT-IRAS spectra of racemic 3MCHO adsorbed at the kinks on the two surfaces. The racemic mixture has no net chirality and thus the spectra obtained from the two surfaces should be identical. The top half of Figure 3 shows the FT-IRAS spectra of rac-3MCHO adsorbed at the kinks on the Cu(643)$^{R/S}$ surfaces and the difference spectrum. The fact is that the two spectra are almost identical, as they should be. The average orientations of the racemic 3MCHO on the two surfaces are identical.

Given the fact that the FT-IRAS spectra of rac-3MCHO adsorbed at the kinks on the Cu(643)$^{R/S}$ surfaces are identical, any differences in the spectra of *R*-3MCHO adsorbed at the kinks on the two surfaces must be attributable to enantiospecific differences in their adsorption geometries. The bottom half of Figure 3 shows the FT-IRAS spectra obtained from *R*-3MCHO adsorbed at the kinks only on the Cu(643)$^{R/S}$ surfaces and the difference spectrum between the two. The region of the spectrum from 1800−2600 cm^{-1} has been removed from the spectrum. The feature that arises from the $\upsilon_{C=O}$ mode is very broad and very weak in the *R*-3MCHO adsorbed only at the kink sites. Although the low intensity of the $\upsilon_{C=O}$ mode in the adsorbed *R*-3MCHO monolayer has been used to conclude that that >C═O bond lies roughly parallel to the plane of the Cu(643) surface, its intensity does not provide any insight into the enantiospecificity of the *R*-3MCHO orientations on the Cu(643)$^{R/S}$ surfaces. The relative intensities of the other modes of *R*-3MCHO are visibly different in the spectra obtained from the two surfaces, and this is clearly indicated by the intensity in the difference spectrum. The fact that this difference spectrum reveals intensity differences in several features indicates that the orientations of *R*-3MCHO on at the *R* and *S* kinks are different or, in other words, that the orientations are enantiospecific.

The differences in the absorption intensities of the *R*-3MCHO adsorbed at the kinks on the Cu(643)$^{R/S}$ surfaces are highlighted in Figure 4, which expands the regions from 1100 to 1450 cm^{-1} and from 2700 to 3050 cm^{-1}. These regions of the spectra are complex, and there are numerous overlapping bands that clearly change in relative intensity. Some appear to shift from one surface to the other, but it is not clear whether this is real or is

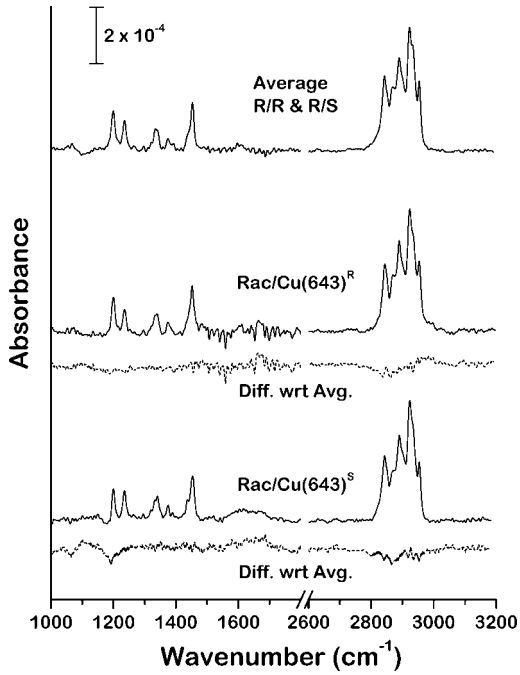

Figure 5. Comparison of the FT-IRAS spectra for racemic 3MCHO on Cu(643)$^{R/S}$ surfaces with the average of the spectra of *R*-3MCHO on the Cu(643)$^{R/S}$ surfaces. The average of the FT-IRAS spectra of R-3MCHO on the Cu(643)$^{R/S}$ surfaces is identical to each of the spectra of racemic 3-MCHO on the Cu(643)$^{R/S}$ surfaces. This indicates that there are no significant interactions between *R*-3MCHO and *S*-3MCHO molecules when the racemic mixture is adsorbed on the Cu(643)$^{R/S}$ surfaces. Spectra are offset for clarity.

simply due to changes in the relative intensities of two unresolved peaks. It is the case, however, that for all of these peaks arising from CH and CC motions, the shifts in frequency are relatively small (<5 cm^{-1}), whereas the changes in relative intensity are comparatively large.

It is worth noting that there is a relationship between the spectra obtained from the *R*-3MCHO and the rac-3MCHO adsorbed at the kinks on the Cu(643)$^{R/S}$ surfaces. The spectrum at the top of Figure 5 is an average of the spectra obtained from *R*-3MCHO adsorbed at the kinks on the Cu(643)^{R} and Cu(643)^{S} surfaces. This is the spectrum that one would expect to obtain from the racemic mixture adsorbed on either surface, assuming that there are no heterochiral interactions between the *R* and *S* enantiomers in the racemic adsorbed mixture that could not occur in the homochiral adsorbed layers. The middle and lower spectra of Figure 5 are those of rac-3MCHO at the kinks on the Cu(643)^{R} surface and rac-3MCHO at the kinks on the Cu(643)^{S} surface. We have already shown in Figure 3 that these are identical. Below each is the difference (dashed line) between the average of the *R*-3MCHO spectra on Cu(643)^{R} and on Cu(643)^{S} and the spectra of rac-3MCHO on either surface. These indicate that the spectra of rac-3MCHO are identical to the average of the *R*-3MCHO spectra on Cu(643)$^{R/S}$. This is not a trivial point, because it indicates that under the conditions of adsorption exposure to the rac-3MCHO really does result in the adsorption of the racemic mixture, rather than the selective adsorption of the species with the higher enantiospecific heat of adsorption. In this experiment, in which we have adsorbed rac-3MCHO at the kinks only, the adsorbate has been exposed to the surface at 320 K using an exposure of 0.15 L, which is sufficient to saturate the kinks. Immediately following adsorption, the sample has been cooled to 120 K to obtain the FT-IRAS spectra. Under these conditions, exposure of the rac-3MCHO does not result in the selective adsorption of one enantiomer. It should be noted that if one used sufficiently high exposures of the chiral surface to rac-3MCHO one ought to observe preferential adsorption of the enantiomer with the greater adsorption energy and thus, an enantioselective separation. Enantioselective separation of rac-3MCHO on the Cu(643)$^{R/S}$ surfaces has been demonstrated in other work.[14]

4. Discussion

In addition to revealing the enantiospecific nature of the *R*-3MCHO orientation on the chiral Cu(643) surfaces, RAIRS also provides insight into how the adsorbed molecules interact with the surface. With 100 monolayers of *R*–3-MCHO on the surface, the $\upsilon_{C=O}$ mode occurred at 1715 cm^{-1}. At a coverage of one monolayer, the $\upsilon_{C=O}$ frequency was red-shifted to 1664 cm^{-1}, indicating that the *R*-3MCHO molecule is bonded to the surface through the carbonyl group. With *R*3MCHO molecules only occupying the kink sites on the surface (0.35 monolayer coverage), the $\upsilon_{C=O}$ mode is absent from the IR spectrum, or at best present as a broad feature at $\sim$1600 cm^{-1}. Surface selection rules, therefore, indicate that the dynamic dipole moment of the $\upsilon_{C=O}$ stretch must lie roughly parallel to the Cu(643) surface and further suggests that the >C═O bond and the plane of the molecular ring are approximately flat on the Cu(643) surface at low coverages. The assertion that *R*-3MCHO is approximately flat on the terraces of the Cu(643) surface is supported by results obtained elsewhere for cyclic compounds adsorbed on high Miller index surfaces. Molecular simulation of the adsorption of 1,2-dimethylcyclohexane on the Pt(854) surface indicates that, at low coverages, the ring is approximately flat on the surface.[11] Both the ideal Pt(854) surface used in those simulations and the Cu(643) surfaces used here have terraces with (111) orientation, long steps with (100) orientation, and short steps with (110) orientation. The long step on the ideal Pt(854) surface is three atomic diameters in length, while the long step on the ideal Cu(643) surface is two atomic diameters in length. Both 3-MCHO and 1,2-dimethylcyclohexane have six-carbon ring structures with two substituent groups bonded to carbon atoms in the ring. Experimental results also indicate that cyclohexane adsorbs to the Cu(111) surface with the ring approximately flat on the surface.[30]

At higher coverages, the orientation of the molecule changed, as shown by the changes in the FT-IRAS spectra as a function of coverage. The intensity of the $\upsilon_{C=O}$ stretch increased by a factor of 5 as the coverage increased to one monolayer. This increase in intensity is larger than would be expected based on the increased number of *R*-3MCHO molecules on the surface and indicates a change in the average orientation of the molecules on the surface. More importantly, the intensity of the $\upsilon_{C=O}$ mode increased relative to the intensity of the CH stretch modes. It is possible that the molecule is tilted with respect to the surface at higher coverages, similar to the behavior of cyclohexane on the Cu(111) surface.[30]

Another interesting result is found by analyzing the IRAS spectra of rac-3MCHO on the Cu(643)$^{R/S}$ surfaces. If the racemic mixture behaved ideally on the Cu(643)$^{R/S}$ surfaces, the IRAS spectrum of the racemic mixture should be an average of the spectra of *R*-3MCHO and *S*-3MCHO on a given chiral surface. Because *S*-3MCHO is not commercially available, it was not possible to perform this comparison. However, the symmetry of this system dictates that the average of the spectra obtained for each enantiomer adsorbed separately on one chiral surface should be equivalent to the average of the spectra obtained for one enantiomer adsorbed

on the two surfaces of opposite chirality. This means that the average of the spectra of *R*-3MCHO on the Cu(643)^R and Cu(643)^S surfaces should be equivalent to the average of the spectra of *R*-3MCHO and *S*-3MCHO on either one of the chiral surfaces. Figure 5 shows the average of the IRAS spectra collected for *R*–3-MCHO on both chiral surfaces. This average spectrum is equivalent to the IRAS spectra of the racemic mixture on either chiral surface. Subtracting the average of the IRAS spectra of the single enantiomer on both chiral surfaces from the IRAS spectra of the racemic mixture on either chiral surface yielded a spectrum of only background noise. In addition to acting as a control experiment, these IRAS spectra show that the average orientation of the racemic mixture on each chiral surface was the average of the orientations of *R*- and *S*-3MCHO on a given chiral surface. There are at least two possible explanations for these results. One possibility is that interactions between adjacent *R* and *S* enantiomers on the surface are not significantly different from the interactions between two *R*-3MCHO molecules or simply that these interactions are very small. Another possibility is that the racemic mixture segregates on the surface into regions containing only a single enantiomer. In that case, *R*- and *S*-3MCHO would only interact at the borders of these regions, minimizing the number of *R*-3MCHO and *S*-3MCHO interactions on the surface. The experiments performed in this work did not differentiate between these two possibilities; however, a technique such as scanning tunneling microscopy should be able to determine whether a racemic mixture segregates into single enantiomer domains on the surface.[31,32]

At first, the results just described might seem to be at odds with the results of a previously published experiment in which the Cu(643)$^{R/S}$ surfaces were used to induce an enantioselective purification of racemic 3MCHO into its enantiomerically purified components.[14] In that experiment racemic 3MCHO was adsorbed at the kinks on the Cu(643)$^{R/S}$ surfaces and then held at ~350 K to allow the selective desorption of one of the two enantiomers into the gas phase, thus leaving an enantiomerically purified adsorbed layer. That purification was the result of a kinetic separation. In this work racemic 3MCHO was adsorbed at 320 K and the FT-IRAS spectra show that this results in the adsorption of a racemic mixture on the surface. If one were to expose the surface to racemic 3MCHO at 320 K for sufficiently long times, the enantiomer with the higher adsorption energy ought to displace the other, thus leading ultimately to a nonracemic or enantiomerically purified mixture on the surface. That purification would be the result of an equilibrium separation. Apparently, at 320 K this occurs very slowly and was not observed in this experiment in which the surface was only exposed to enough 3MCHO to saturate the kinks at 320 K.

Ideally, one would like to use the FT-IRAS spectra obtained in this work to determine the adsorption geometry of *R*-3MCHO at the chiral kink sites on the Cu(643)$^{R/S}$ surfaces and, in particular, to identify differences in the orientations that lead to the observed differences in the intensities in the FT-IRAS spectra. Ultimately, of course, this would serve as the basis for beginning to understand the origins of the differences in the heats of adsorption of *R*-3MCHO on the Cu(643)$^{R/S}$ surfaces and the origins of enantioselectivity.[14] The intensity change and the frequency shift of the $\upsilon_{C=O}$ mode has been used to suggest that it is the >C=O group that interacts with the surface most strongly and that it lies roughly parallel to the surface. Further analysis of the spectra and the vibrational mode intensities has not been attempted. In part, this is because the vibrational spectrum of a molecule such as *R*-3MCHO is quite complicated, and it is not clear how well one could assign all the modes observed in the spectra of the adsorbed molecule. Second, one has to bear in mind the fact that the surface itself is quite complex in structure and that thermal roughening of the surface results in a structure that is highly nonideal.[20] On the real, thermally roughened surface, one has kinks occurring at the intersections of step edges of a variety of lengths rather than single atom kinks distributed uniformly along the step edge as shown in figure 1. In other words, the real thermally roughened surface exposes many different types of kinks. The breadth of the $\upsilon_{C=O}$ feature at 1600 cm^{-1} in the "kinks only" spectrum of figure 2 is a likely indication of inhomogeneous broadening arising from adsorption at kinks with a variety of different structures. Thus, the intensities of the vibrational modes observed in spectra obtained from *R*-3MCHO adsorbed at chiral kinks merely reflect the average orientation of a set of molecules adsorbed at a variety of kinks types. That being the case, one cannot easily analyze the spectra to obtain a single, meaningful orientation for 3-MCHO adsorbed at the kink sites.

5. Conclusions

R-3MCHO adopts enantiospecific orientations on the Cu(643)^R and Cu(643)^S surfaces. These enantiospecific orientations resulted in enantiospecific differences in desorption energies, as seen previously.[14] As with the TPD results for *R*-3MCHO on Cu(643)$^{R/S}$, enantiospecific effects were only observed for molecules adsorbed at the kink sites on the Cu(643)$^{R/S}$ surfaces.

Acknowledgment. The authors would like to acknowledge support from the National Science Foundation through Grant No. CTS-0216170.

References and Notes

(1) McFadden, C. F.; Cremer, P. S.; Gellman, A. J. *Langmuir* **1996**, *12*, 2483–7.
(2) Ahmadi, A.; Attard, G. *Langmuir* **1999**, *15*, 2420–2424.
(3) Sholl, D. S.; Asthagiri, A.; Power, T. D. *J. Phys. Chem. B* **2001**, *105* (21), 4771–4782.
(4) Attard, G. *J. Phys. Chem. B* **2001**, *105* (16), 3158–3167.
(5) Attard, G.; Ahmadi, A.; Feliu, J.; Rodes, A.; Herrero, E.; Blais, S.; Jerkiewicz, G. *J. Phys. Chem. B* **1999**, *103*, 1381–5.
(6) Gellman, A. J.; Horvath, J. D.; Buelow, M. T. *J. Mol. Catal., A* **2001**, *167*, 3–11.
(7) Horvath, J. D.; Gellman, A. J. *J. Am. Chem. Soc.* **2001**, *123*, 7953–7954.
(8) Horvath, J. D.; Gellman, A. J. *J. Am. Chem. Soc.* **2002**, *124*, 2384–2392.
(9) Horvath, J. D.; Gellman, A. J.; Sholl, D. S.; Power, T. D. Enantiospecific Properties of Chiral Single-Crystal Surfaces. In *Chirality: Physical Chemistry*; Hicks, J., Ed.; Oxford University Press: Washington, DC, 2002; pp 269−282.
(10) Power, T. D.; Sholl, D. S. *J. Vac. Sci. Technol. A* **1999**, *17*, 1700–4.
(11) Power, T. D.; Sholl, D. S. *Top. Catal.* **2002**, *18* (3−4), 201–208.
(12) Sholl, D. S. *Langmuir* **1998**, *14*, 862–7.
(13) Watson, D. J.; Attard, G. A. *Electrochim. Acta* **2001**, *46*, 3157–3161.
(14) Horvath, J.; Kamakoti, P.; Koritnik, A.; Sholl, D. S.; Gellman, A. J. *J. Am. Chem. Soc.* **2004**, *126* (45), 14998–14994.
(15) Horvath, J. D.; Gellman, A. J. *Top. Catal.* **2003**, *25* (1−4), 9–15.
(16) Greber, T.; Sljivancanin, Z.; Schillinger, R.; Wider, J.; Hammer, B. *Phys. Rev. Lett.* **2006**, *96*, (5).
(17) Bhatia, B.; Sholl, D. S. *Angew. Chem., Int. Ed.* **2005**, *44* (47), 7761–7764.
(18) Rankin, R. B.; Sholl, D. S. *J. Chem. Phys.* **2006**, *124* (7), 74703.
(19) Sljivancanin, Z.; Gothelf, K. V.; Hammer, B. *J. Am. Chem. Soc.* **2002**, *124* (49), 14789–14794.
(20) Power, T. D.; Asthagiri, A.; Sholl, D. S. *Langmuir* **2002**, *18*, 3737–3748.

(21) Pouchert, C. J. *The Aldrich Library of Infrared Spectra*, 3rd ed.; Aldrich Chemical Company: Milwaukee, WI, 1981.
(22) Forel, M. T.; Petrissans, J. *J. Chim. Phys.* **1966**, *63* (4), 625–634.
(23) Devlin, F. J.; Stephens, P. J. *J. Phys. Chem.* **1999**, *103*, 527–538.
(24) Fuhrer, H. *Chem. Rev.* **1972**, *72* (5), 439–456.
(25) Syomin, D.; Koel, B. *Surf. Sci.* **2002**, *498* (1−2), 53–60.
(26) Lavoie, S.; McBreen, P. *J. Phys. Chem. B* **2005**, *109* (24), 11986–11990.
(27) Asthagiri, A.; Feibelman, P. J.; Sholl, D. S. *Top. Catal.* **2002**, *18* (3−4), 193–200.
(28) Power, T. D.; Asthagiri, A.; Sholl, D. S. *Langmuir* **2002**, *18* (9), 3737–3748.
(29) Giesen, M.; Dieluweit, S. *J. Mol. Catal., A* **2004**, *216*, 263–272.
(30) Raval, R.; Parker, S. F.; Chesters, M. A. *Surf. Sci.* **1993**, *289*, 227–236.
(31) Eckhardt, C. J.; Peachy, N. M.; Swanson, D. R.; Takacs, J.; Khan, M. A.; Gong, X.; Kim, J. H.; Wang, J.; Uphaus, R. A. *Nature* **1993**, *362* (6421), 614–616.
(32) Fang, H.; Giancarlo, L. C.; Flynn, G. W. *J. Phys. Chem. B* **1998**, *102* (38), 7311–7315.

JP0753878